

Modulation of p-type units in tripodal bipolar hosts towards highly efficient red phosphorescent OLEDs

Quan Ran¹, Yuan-Lan Zhang¹, Xiaochen Hua, Man-Keung Fung, Liang-Sheng Liao*, Jian Fan**

Jiangsu Key Laboratory for Carbon-Based Functional Materials & Devices, Institute of Functional Nano & Soft Materials (FUNSOM), Joint International Research Laboratory of Carbon-Based Functional Materials and Devices, Soochow University, Suzhou, Jiangsu, 215123, China

ABSTRACT

Three novel tripodal bipolar compounds (CNTPA-CZ, CNTPA-PXZ and CNTPA-PTZ) were designed and synthesized, where three functional groups were attached to 1,3,5-positions of the central benzene ring, respectively. In these three compounds, carbazole/phenoxazine/phenothiazine (CZ/PXZ/PTZ) and benzonitrile were applied as electron-donating and electron-withdrawing groups, respectively, to achieve bipolar transport functionality, which was confirmed by the hole-only and electron-only device results. Due to the efficient energy transfer from these compounds to the dopant (Ir(MDQ)₂(acac)), the red phosphorescent OLEDs demonstrated high device performance with maximum external quantum efficiency (EQE) over 20%. Particularly, the red OLED hosted by CNTPA-PTZ achieved a maximum efficiency of 42.5 cd/A, 44.3 lm/w and 23.4% with the EQE roll-off ratio of 3.4% from the peak value to that at a brightness of 500 cd/m².

1. Introduction

Since organic light-emitting diode (OLED) was reported by C. W. Tang and S. A. VanSlyke in 1987 [1], tremendous progress has been made in OLED, which has demonstrated practical application in display and lighting device [2–14]. OLED has caught both academic and industrial attention due to its superior inherent properties such as slim structure, low weight, wide viewing angle and fast response time. Generally the emission layer (EML) is a blend of host and dopant material, and the dopant molecules are finely dispersed in the host matrix. The use of the host-guest strategy is necessary for suppressing the detrimental triplet–triplet annihilation process [15–17]. So host materials play an important role in the development of highly efficient and stable OLED. To ensure the efficient energy transfer from host to dopant, the host materials should possess triplet energy higher than that of dopant, suitable frontier molecular orbital (FMO) energy level and good charge transport ability [18–21].

Within a traditional OLED device, the holes and electrons are injected from the electrodes, transported via the interfacial layers and eventually combined in the emission layer (EML) to emit light. The bipolar host materials can transport both holes and electrons and increase the opportunity for hole and electron recombination in the EML, which usually results in high quantum efficiency and low efficiency roll-off in phosphorescent organic light-emitting diodes (PHOLEDs) [22–25]. During last decade much efforts have been devoted to the

development of bipolar hosts [26–34]. The bipolar functionality of host materials can be realized with either single-component organic compound or two-component system. For example, Kim et al. reported a novel exciplex forming cohost composed of a representative hole-transporting material NPB (N,N'-diphenyl-N,N'-bis(1,1'-biphenyl)-4,4'-diamine) and a typical electron-transporting material PO-T2T (5-triazine-2,4,6-triyl)tris(benzene-3,1-diyI)tris(diphenylphosphine oxide). The red-emitting PhOLEDs based on this exciplex host achieved a maximum EQE of 34.1% and power efficiency of 62.2 lm/W [35]. In case of single-component system, the host materials are generally decorated with electron-donating and electron-withdrawing groups to facilitate the hole and electron transport, respectively [36].

So far many popular host materials have been developed [37–41]. For instance, the carbazole derivative 1,3-bis(N-carbazolyl)benzene (mCP) has been widely used as host material. However, it has a low glass transition temperature (55 °C) [42], leading to the morphological instability [43]. In addition, due to the lack of electron-withdrawing group in mCP, it's difficult to achieve the balanced ratio of holes and electrons in the mCP-hosted OLED. Recently, lots of mCP derivatives have been developed as host materials, and usually they were functionalized with electron-poor group to optimize the recombination properties in the EML [44–47]. For example, Lee et al. modified mCP core with diphenylphosphine oxide functional group to obtain bipolar charge-transport properties [48]. Kippelen and coworkers applied sulfone–mCP host material for highly efficient OLED and achieved current

* Corresponding author.

** Corresponding author.

E-mail addresses: lsiao@suda.edu.cn (L.-S. Liao), jianfan@suda.edu.cn (J. Fan).

¹ The two authors contribute equally to this paper.

efficiency more than 81 cd/A and EQE of 26.5% with the thermally activated delayed fluorescence (TADF) material as the emitter [49]. In this work, the electron-deficient group benzonitrile was introduced into mCP derivatives to produce the tripodal host materials and at the same time to tune the charge-transport properties in the emissive region. Furthermore, we also study the effect of variation of electron-donating group on the electronic structures of the host materials and the device performance via changing the carbazole group to phenoxazine and phenothiazine. Thus three host materials (CNTPA-CZ, CNTPA-PXZ and CNTPA-PTZ) were designed and synthesized, and they demonstrated high thermal stability with glass transition temperature in the range of 99–121 °C. The red OLEDs hosted by these compounds showed high quantum efficiency over 20%. Remarkably, the CNTPA-PTZ-hosted red OLEDs respectively yielded the maximum EQEs of 23.4%, and 22.6% at 500 cd/m² due to the good hole and electron transport capability.

2. Experimental section

2.1. Materials and methods

All chemicals and reagents were used as received from commercial sources without further purification. ¹H NMR and ¹³C NMR spectra were obtained on a Bruker 400 spectrometer and Agilent DD2-600 MHz NMR spectrometer. Matrix-Assisted Laser Desorption/Ionization Time of Flight Mass Spectrometry (MALDI-TOF-MS) was measured with a BRUKER ultrafleXtreme MALDI-TOF spectrometer. Ultraviolet–visible (UV–vis) absorption spectra were obtained on a Hitachi U-3900 UV–Vis spectrophotometer. PL spectra and phosphorescent spectra were obtained on a Hitachi F-4600 fluorescence spectrophotometer. Thermogravimetric analysis (TGA) was performed on a TA SDT 2960 instrument at a heating rate of 10 °C/min under nitrogen. Differential scanning calorimetry (DSC) was performed on a TA DSC 2010 unit at a heating rate of 10 °C/min under nitrogen. Cyclic voltammetry (CV) was carried out on a CHI600 voltammetric analyzer at room temperature with ferrocenium-ferrocene (Fc⁺/Fc) as the internal standard. A conventional three-electrode configuration consisting of a Pt-wire counter electrode, an Ag/AgCl reference electrode, and a platinum working electrode was used. The oxidative scans were performed at a scan rate of 0.05 V/s. Degassed DCM was used as solvent for oxidation scan with tetrabutylammonium hexafluorophosphate (TBAPF₆) (0.1 M) as the supporting electrolyte.

2.2. Device fabrication and measurements

The OLED devices were fabricated through vacuum deposition on commercial pre-patterned ITO-coated glass substrates (135 nm, 31.9 mm × 31.9 mm × 0.7 mm) with the sheet resistance of 15 Ω per square under high vacuum of 4 × 10⁻⁶ Torr. The active area of each device is 0.09 cm². The ITO substrates were cleaned by sonication in Decon, ethanol, and deionized water for 10 min subsequently, then dried in an oven at 110 °C and treated by UV ozone for 15 min. The deposition rate were controlled at 0.3–0.4 Å/s for HAT-CN, 0.2–0.4 Å/s for Liq, 1–2 Å/s for other organic layers and 6–8 Å/s for Al anode. The EL spectra, CIE coordinates, J–V–L curves, CE and PE of the devices were measured with a programmable spectra scan photometer (PHOTO RESEARCH, PR 655) and a constant current source meter (KEITHLEY 2400) at room temperature.

2.3. Synthesis of 4-(phenylamino)benzonitrile

A mixture of aniline (5.12 g, 55 mmol), 4-bromobenzonitrile (10 g, 55 mmol), tris(dibenzylideneacetone)dipalladium (504 mg, 0.55 mmol), 2-dicyclohexylphosphino-2',6'-dimethoxy-1,1'-biphenyl (452 mg, 1.1 mmol) and sodium tert-butoxide (10.6 g, 110 mmol) in 300 ml of toluene were heated at 80 °C overnight under argon. After cooling down to room temperature, the mixture was extracted with dichloromethane.

The combined organic extracts were dried over Na₂SO₄ and evaporated under reduced pressure. The crude product was purified by column chromatography on silica gel using petroleum ether/dichloromethane (PE/DCM, 8/1, v/v) as the eluent to afford the target compound (8 g, 75%). ¹H NMR (400 MHz, CDCl₃) δ 7.48 (d, *J* = 8.6 Hz, 2H), 7.36 (t, *J* = 7.8 Hz, 2H), 7.17 (d, *J* = 7.8 Hz, 2H), 7.12 (t, *J* = 7.4 Hz, 1H), 6.97 (d, *J* = 8.7 Hz, 2H), 6.10 (s, 1H).

2.4. Synthesis of 9,9'-(5-chloro-1,3-phenylene)bis(9H-carbazole)

A mixture of 1,3-dibromo-5-chlorobenzene (2 g, 7.41 mmol), 9H-carbazole (2.60 g, 15.56 mmol), tris(dibenzylideneacetone)dipalladium (339 mg, 0.37 mmol), 2-dicyclohexylphosphino-2',6'-dimethoxy-1,1'-biphenyl (457 mg, 1.11 mmol) and sodium tert-butoxide (2.85 g, 29.64 mmol) in 100 ml of toluene were heated at 80 °C for 4 h under argon. After cooling down to room temperature, the mixture was extracted with dichloromethane. The combined organic extracts were dried over Na₂SO₄ and evaporated under reduced pressure. The crude product was purified by column chromatography on silica gel using petroleum ether/dichloromethane (PE/DCM, 8/1, v/v) as the eluent to afford the target compound (2.46 g, 75%). ¹H NMR (400 MHz, CDCl₃) δ 8.15 (d, *J* = 7.7 Hz, 4H), 7.76 (s, 1H), 7.72 (d, *J* = 1.6 Hz, 2H), 7.55 (d, *J* = 8.2 Hz, 4H), 7.46 (t, *J* = 7.6 Hz, 4H), 7.33 (t, *J* = 7.4 Hz, 4H).

10,10'-(5-chloro-1,3-phenylene)bis(10H-phenoxazine) and 10,10'-(5-chloro-1,3-phenylene)bis(10H-phenothiazine) were synthesized according to the same procedure as for 9,9'-(5-chloro-1,3-phenylene)bis(9H-carbazole).

10,10'-(5-chloro-1,3-phenylene)bis(10H-phenoxazine): ¹H NMR (600 MHz, CDCl₃) δ 7.51 (s, 2H), 7.34 (s, 1H), 6.70 (dt, *J* = 7.1 Hz, 12H), 6.04 (d, *J* = 7.6 Hz, 4H).

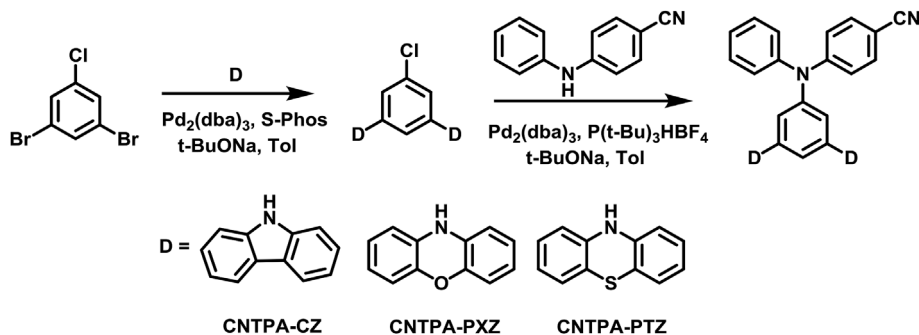
10,10'-(5-chloro-1,3-phenylene)bis(10H-phenothiazine): ¹H NMR (400 MHz, CDCl₃) δ 7.19 (d, *J* = 7.4 Hz, 4H), 7.14 (s, 2H), 7.07 (t, *J* = 7.4 Hz, 4H), 6.99 (q, *J* = 7.4 Hz, 5H), 6.72 (d, *J* = 8.0 Hz, 4H).

2.5. Synthesis of 4-((3,5-di(9H-carbazol-9-yl)phenyl)(phenyl)amino)benzonitrile (CNTPA-CZ)

A mixture of 9,9'-(5-chloro-1,3-phenylene)bis(9H-carbazole) (1.05 g, 2.37 mmol), 4-(phenylamino)benzonitrile (551 mg, 2.84 mmol), tris(dibenzylideneacetone)dipalladium (109 mg, 0.12 mmol), tri-*t*-butylphosphonium tetrafluoroborate (104 mg, 0.36 mmol) and sodium tert-butoxide (910 mg, 9.48 mmol) in 100 ml of toluene were heated at 110 °C overnight under nitrogen. After cooling down to room temperature, the mixture was extracted with dichloromethane. The combined organic extracts were dried over Na₂SO₄ and evaporated under reduced pressure. The crude product was purified by column chromatography on silica gel using petroleum ether/dichloromethane (PE/DCM, 1/1, v/v) as the eluent to afford a white solid (1.05 g, 74%). ¹H NMR (600 MHz, CDCl₃) δ 8.13 (d, *J* = 7.7 Hz, 4H), 7.60 (s, 1H), 7.57 (d, *J* = 8.5 Hz, 2H), 7.51 (d, *J* = 8.2 Hz, 4H), 7.44 (dt, *J* = 7.9 Hz, 6H), 7.40 (s, 2H), 7.31 (tt, *J* = 7.8 Hz, 9H). ¹³C NMR (151 MHz, CDCl₃) δ 150.72, 149.09, 145.54, 140.31, 140.10, 133.52, 130.25, 126.53, 126.15, 123.69, 121.72, 120.79, 120.54, 120.52, 119.71, 119.14, 109.57, 104.79. MALDI-TOF-MS: *m/z*: calcd for C₄₃H₂₈N₄: 600.73, found: 600.02. Anal. calcd for C₄₃H₂₈N₄ (%): C 85.97, H 4.70, N 9.33; found: C 85.83, H 5.07, N 9.73.

4-((3,5-di(10H-phenoxazin-10-yl)phenyl)(phenyl)amino)benzonitrile (CNTPA-PXZ) and 4-((3,5-di(10H-phenothiazin-10-yl)phenyl)(phenyl)amino)benzonitrile (CNTPA-PTZ) were prepared with the same procedure as for CNTPA-CZ.

CNTPA-PXZ: ¹H NMR (600 MHz, CDCl₃) δ 7.49 (d, *J* = 8.7 Hz, 2H), 7.38 (t, *J* = 7.8 Hz, 2H), 7.19 (d, *J* = 8.5 Hz, 5H), 7.14–7.08 (m, 3H), 6.69 (s, 12H), 6.08 (dd, *J* = 3.2 Hz, 4H). ¹³C NMR (151 MHz, CDCl₃) δ 151.13, 150.40, 145.25, 143.96, 142.63, 133.54, 130.28, 127.86, 126.38, 126.20, 125.89, 123.29, 121.94, 121.76, 119.02, 115.85, 112.84, 104.98. MALDI-TOF-MS: *m/z*: calcd for C₄₃H₂₈N₄O₂: 632.72,



Scheme 1. The synthetic route of CNTPA-CZ, CNTPA-PXZ and CNTPA-PTZ.

found: 632.18. Anal. calcd for $C_{43}H_{28}N_4O_2$ (%): C 81.63, H 4.46, N 8.86; found: C 81.72, H 4.35, N 8.79.

CNTPA-PTZ: 1H NMR (400 MHz, $CDCl_3$) δ 7.45 (d, $J = 8.6$ Hz, 2H), 7.35 (t, $J = 7.7$ Hz, 2H), 7.18 (t, $J = 8.5$ Hz, 3H), 7.10 (t, $J = 9.7$ Hz, 6H), 7.00 (t, $J = 7.4$ Hz, 4H), 6.93 (dd, $J = 7.6$ Hz, 7H), 6.59 (d, $J = 8.0$ Hz, 4H). ^{13}C NMR (151 MHz, $CDCl_3$) δ 150.66, 149.57, 145.46, 145.19, 143.05, 133.31, 130.04, 127.47, 126.98, 126.43, 125.86, 124.21, 123.71, 121.26, 119.90, 119.71, 119.27, 118.68, 104.12. MALDI-TOF-MS: m/z : calcd for $C_{43}H_{28}N_4S_2$: 664.85, found: 664.14. Anal. calcd for $C_{43}H_{28}N_4S_2$ (%): C 77.68, H 4.25, N 8.43; found: C 77.44, H 4.44, N 8.25.

3. Results and discussion

3.1. Preparation and characterization

The synthetic routes of CNTPA-CZ, CNTPA-PXZ and CNTPA-PTZ were described in Scheme 1. These compounds were prepared via Buchwald-Hartwig cross-coupling reaction between the corresponding chloride and 4-(phenylamino)benzonitrile with $Pd_2(dba)_3$ as the catalyst in decent yields. The complexes were fully characterized by 1H and ^{13}C NMR (Figure S1-Figure S10), MALDI-TOF mass spectrometry and elemental analysis. CNTPA-CZ, CNTPA-PXZ and CNTPA-PTZ demonstrated good thermal stabilities with the decomposition temperatures (corresponding to 5% weight loss) of 427 °C, 408 °C and 428 °C, respectively (Fig. 1). As shown in Fig. 2, CNTPA-CZ (121 °C) showed higher glass transition temperature than those of CNTPA-PXZ (104 °C) and CNTPA-PTZ (99 °C), probably due to the rigidity of CNTPA-CZ.

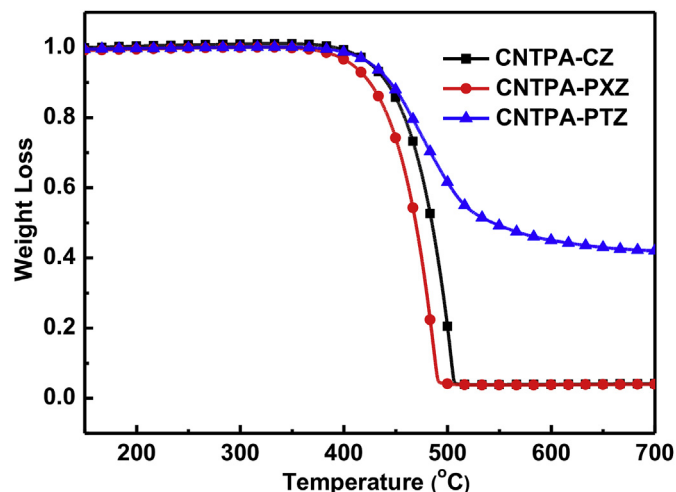


Fig. 1. The TGA curves of CNTPA-CZ, CNTPA-PXZ and CNTPA-PTZ at a heating rate of 10 °C/min under N_2 .

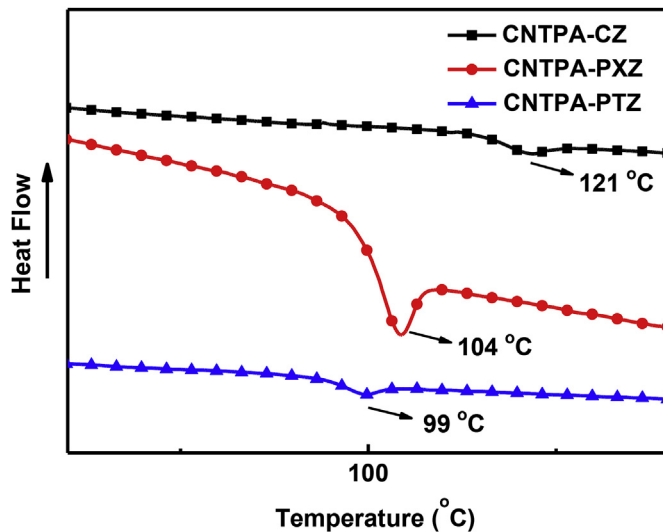


Fig. 2. The DSC thermograms of CNTPA-CZ, CNTPA-PXZ and CNTPA-PTZ at a heating rate of 10 °C/min under N_2 .

3.2. Photophysical properties

The absorption spectra, fluorescence spectra of CNTPA-CZ, CNTPA-PXZ and CNTPA-PTZ were recorded in toluene at room temperature (RT), and phosphorescence spectra in toluene at 77 K (Fig. 3). CNTPA-CZ showed structured absorption band around 330 nm, which could be assigned to carbazole-based absorption [48]. The broad and structureless absorption band over 300 nm observed in absorption spectra of CNTPA-PXZ and CNTPA-PTZ could be assigned to phenoxazine and phenothiazine-based absorption, respectively [50]. Due to the strong electron-donating ability of phenoxazine and phenothiazine, CNTPA-PXZ and CNTPA-PTZ showed a red-shift (around 10 nm) in their absorption spectra relative to that of CNTPA-CZ. Thus both CNTPA-PXZ and CNTPA-PTZ had smaller bandgaps than CNTPA-CZ. No obvious intramolecular charge transfer (ICT) absorption was observed for all the three compounds. As shown in Fig. S11, these compounds essentially showed solvent polarity-independent absorption properties, indicating that there was no strong ICT in the ground state. However, strong solvent polarity-dependent emission behavior was observed for these compounds (Fig. S12), suggesting that there was a certain degree of ICT in their excited state [51]. The photoluminescence quantum yield (PLQY) of Ir(MDQ) $_2$ (acac) doped in CNTPA-CZ, CNTPA-PXZ and CNTPA-PTZ host materials were measured with an integrating sphere to be 0.615, 0.718 and 0.845, respectively (Table S1). The singlet/triplet energy values of CNTPA-CZ (3.11/2.76 eV), CNTPA-PXZ (2.86/2.73 eV) and CNTPA-PTZ (2.74/2.45 eV) were estimated from the emission peaks in their fluorescence spectra and phosphorescence spectra, respectively. Since the triplet energy of Ir(MDQ) $_2$ (acac) is around 2.0 eV

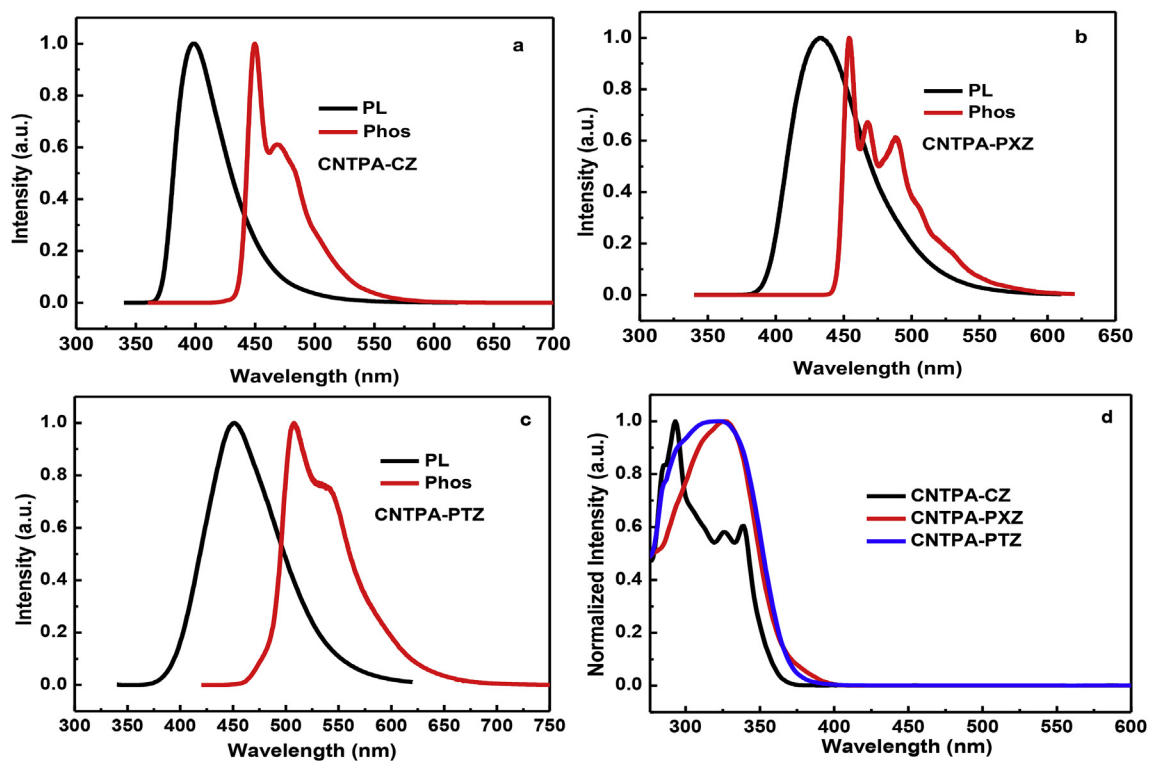


Fig. 3. The fluorescence spectra in toluene at room temperature (RT) and phosphorescence spectra in toluene at 77 K of (a) CNTPA-CZ, (b) CNTPA-PXZ, (c) CNTPA-PTZ and the absorption spectra of these compounds in toluene at RT (d).

[52], these compounds could be used as host materials for this red emitter in PHOLEDs, and the relatively large triplet-triplet energy difference between host and dopant would prohibit the reverse energy transfer from dopant to host, which could lead to the low efficiency roll-off at high luminance.

The electrochemical behavior of these compounds were studied by the cyclic voltammetry (CV) measurement in degassed DCM (Fig. 4). HOMOs of these compounds were estimated from their onset oxidation potential vs Fc^+/Fc with the equation $E_{\text{HOMO}} = -4.8 - E_{\text{ox}}$ [53]. Due to the absence of reduction peak in the cyclic voltammetry curves,

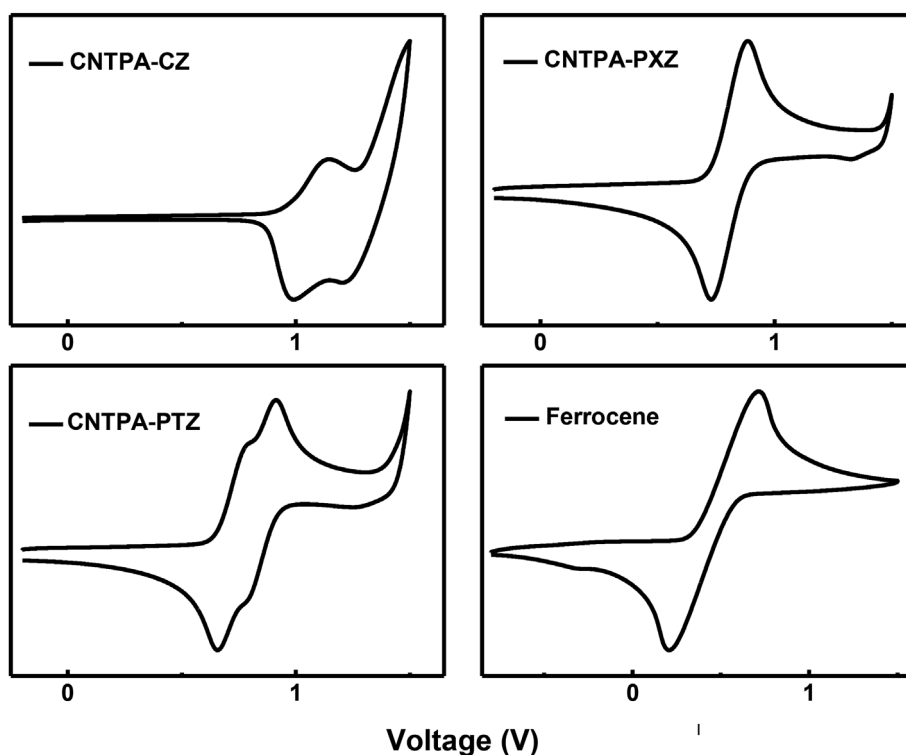


Fig. 4. Cyclic voltammograms of CNTPA-CZ, CNTPA-PXZ and CNTPA-PTZ in DCM for oxidation.

Table 1
Physical properties of CNTPA-CZ, CNTPA-PXZ and CNTPA-PTZ.

Compounds	T_g [°C]	T_d [°C]	S_1 [eV]	T_1 [eV]	ΔE_{ST} [eV]	HOMO [eV]	LUMO [eV]	E_g [eV]
CNTPA-CZ	121	427	3.11	2.76	0.35	-5.29	-1.82	3.47
CNTPA-PXZ	104	408	2.86	2.73	0.13	-5.06	-1.67	3.39
CNPXZ-PTZ	99	428	2.74	2.45	0.29	-4.99	-1.62	3.37

E_g = energy gap calculated from the onset absorption wavelength; HOMO estimated by cyclic voltammetry, LUMO deduced from E_g and HOMO; T_d = temperature for 5% weight loss; T_g = glass-transition temperature.

their LUMOs were calculated with the difference between HOMO and the corresponding optical bandgap. The HOMO and LUMO energy levels of these compounds were summarized in Table 1. The HOMO energy levels of CNTPA-PXZ and CNTPA-PTZ were much higher than that of CNTPA-CZ since the phenoxazine and phenothiazine were stronger electron-donating groups than carbazole unit, which was consistent with the reported results [54]. Considering that all these three compounds contained the same electron-withdrawing group, it's not surprising that CNTPA-CZ had the largest bandgap among the three compounds.

3.3. DFT calculations

In order to understand the photophysical properties and electronic structure of these three hosts, density functional theory (DFT) calculations were carried out. Fig. 5 indicated that the HOMOs were mainly located on the CZ, PXZ and PTZ units for CNTPA-CZ, CNTPA-PXZ and CNTPA-PTZ, respectively. LOMOs of these compounds were mainly distributed on the benzonitrile and the central benzene motif. Due to the small steric hindrance between carbazole and the central benzene, the HOMO in CNTPA-CZ was partially located on the central benzene group. DFT calculation also confirmed that CNTPA-CZ had the lowest HOMO energy levels among these compounds and all the compounds had the similar LUMO energy levels. To better understand the natures of the singlet excited state, it is useful to refer to the natural transition orbitals (NTO) analysis (Fig. S13) [55]. For CNTPA-PXZ and CNTPA-PTZ, their NTO hole and electron wavefunctions were mainly distributed on the PXZ/PTZ donor and benzonitrile acceptor moieties, respectively. For CNTPA-CZ, the NTO hole wavefunction was mainly confined on the central benzene and CZ group, and NTO electron was

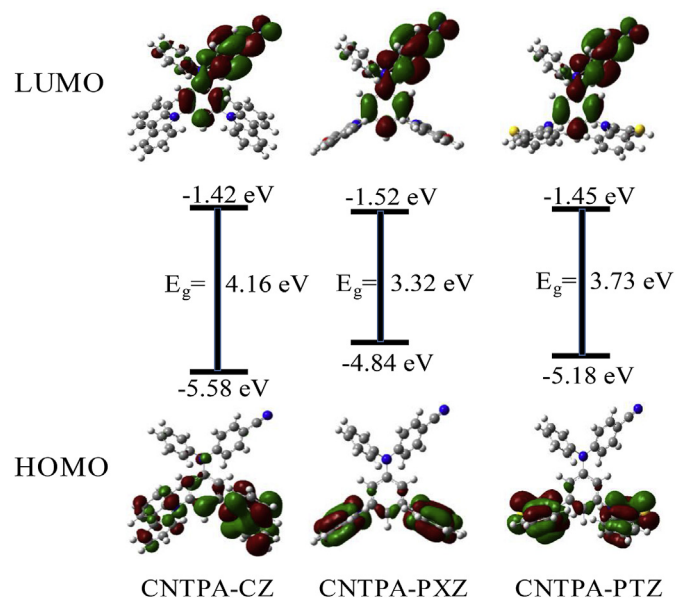


Fig. 5. Theoretically calculated spatial distributions of CNTPA-CZ, CNTPA-PXZ and CNTPA-PTZ.

on benzonitrile. So the singlet excited state of these compounds had charge-transfer character, agreeing well with the observation of their solvent-polarity dependent emission behaviors.

3.4. Electroluminescence properties

To investigate the potential of CNTPA-CZ, CNTPA-PXZ and CNTPA-PTZ as host materials, red PHOLEDs were fabricated with typical device structure as follows: ITO/HAT-CN (10 nm)/TAPC (50 nm)/Host: Ir(MDQ)₂(acac) (20 nm)/TPBi (55 nm)/LiQ (2 nm)/Al (120 nm). These hosts were doped with Ir(MDQ)₂(acac) to form the emitting layer (EML). HAT-CN (dipyrazino[2,3-f:2',3'-h]quinoxaline-2,3,6,7,10,11-hexacarbonitrile) was used as hole injection layer (HIL), and LiQ (8-hydroxyquinolinolato lithium) as electron injection layer (EIL). TAPC (1,1-bis[4-[N,N-di(p-tolyl)-amino]phenyl]cyclohexane) was used as hole transport layer (HTL), and TPBi 1,3,5-tris(N-phenylbenzimidazol-2-yl)benzene as electron transport layer (ETL). The performance of these red PHOLEDs were summarized in Table 2.

The energy levels of the materials used in the red OLEDs were depicted in Fig. 6. CNTPA-PXZ and CNTPA-PTZ had shallower HOMO levels than that of CNTPA-CZ, leading to the enhanced hole-injection from hole transport layer, which could result in the low driving voltages in their hosted device [56]. The current density-voltage-luminance (J - V - L) characteristics, current efficiency (CE)-, power efficiency (PE)-, and external quantum efficiency (EQE)-luminance curves, electroluminescence (EL) spectra of devices are included in Figs. 7–9. At the relatively low doping levels (2.5%–4%) of Ir(MDQ)₂(acac), these hosts based red OLED showed high device performance with the maximum EQE over 20%. For CNTPA-CZ hosted device, the maximum power efficiency was 25.9 lm/W; while for CNTPA-PXZ and CNTPA-PTZ based devices, the maximum power efficiencies were 39.7 lm/W and 44.3 lm/W, respectively. The high power efficiencies observed in CNTPA-PXZ and CNTPA-PTZ based devices were probably due to their low driving voltages. CNTPA-PTZ based device showed the maximum power efficiency and EQE of 44.3 lm/W and 23.4%, respectively, maintaining an EQE over 21% at 1000 cd/m², compared to 19.1% at 1000 cd/m² for the CNTPA-CZ based device. Notably, CNTPA-CZ-, CNTPA-PXZ-, and CNTPA-PTZ-based devices exhibited relatively low EQE roll-off values of 5.9, 12.4, and 8.5%, respectively, from the peak value to that at a brightness of 1000 cd/m². Hole-only and electron-only devices of CNTPA-CZ, CNTPA-PXZ and CNTPA-PTZ were fabricated to study their hole/electron-injection and -transport properties [48]. The hole current densities of CNTPA-PXZ and CNTPA-PTZ were much higher than that of the CNTPA-CZ, indicating better hole-injection and -transport properties of CNTPA-PXZ and CNTPA-PTZ (Fig. S14); while the three compounds showed similar electron-injection and -transport properties. So these compounds showed good bipolar charge transport properties, which is beneficial in broadening the recombination zone of the emitting layer.

4. Conclusion

In conclusion, three tripodal bipolar host materials CNTPA-CZ, CNTPA-PXZ and CNTPA-PTZ were prepared and applied in red PHOLEDs. The electron-donating carbazole group in CNTPA-CZ was

Table 2
Electroluminescence characteristics of the devices.

Device	V _{on} ^a (V)	CE ^b [cd/A]	PE ^b [lm/W]	EQE ^b [%]	CIE ^c (x, y)
CNTPA-CZ	4.27	34.5, 34.1, 32.9	25.9, 21.3, 18.7	20.3, 19.8, 19.1	(0.61, 0.39)
CNTPA-PXZ	3.24	40.5, 37.7, 35.8	39.7, 31.4, 27.2	21.8, 20.3, 19.1	(0.59, 0.40)
CNTPA-PTZ	3.04	42.5, 40.8, 38.9	44.3, 36.5, 31.6	23.4, 22.6, 21.4	(0.60, 0.40)

^a Turn-on voltage (V_{on}) at 100 cd/m².

^b Current efficiency (CE), power efficiency (PE) or external quantum efficiency (EQE) in the order of maximum, at 500 cd/m² and at 1000 cd/m².

^c Commission International de l'Eclairage coordinates measured at 5 mA/cm².

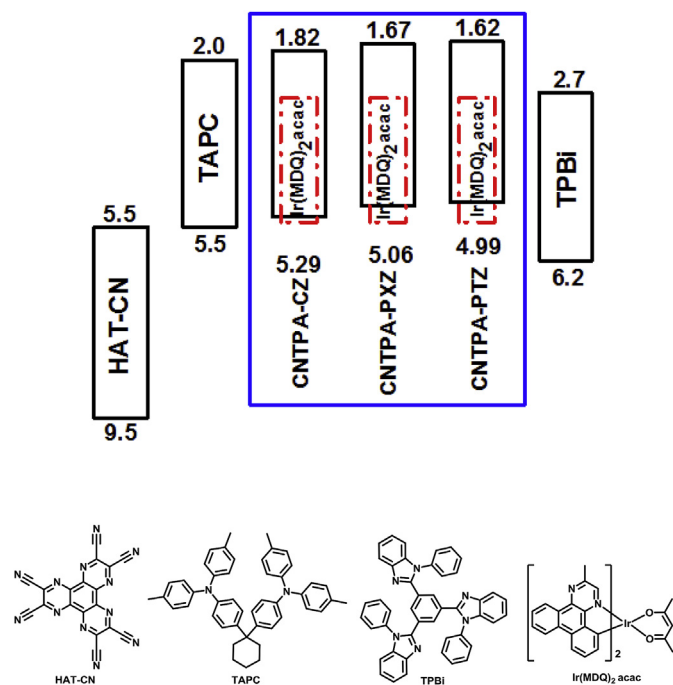


Fig. 6. Energy levels and chemical structures of the materials employed in the devices.

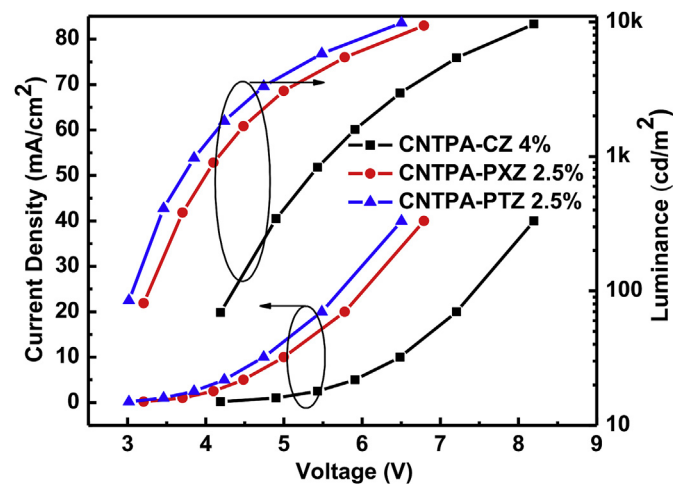


Fig. 7. The current density-voltage-luminance curves.

replaced by phenoxazine and phenothiazine to yield CNTPA-PXZ and CNTPA-PTZ, respectively. The incorporation of heteroatoms (O and S) to break the π -conjugation and to increase the electron-donating capability could change the optoelectronic properties of these materials. As a result, CNTPA-PXZ and CNTPA-PTZ showed higher HOMO energy levels, lower driving voltages, higher hole transport capability and better device performance than CNTPA-CZ. The CNTPA-PTZ hosted

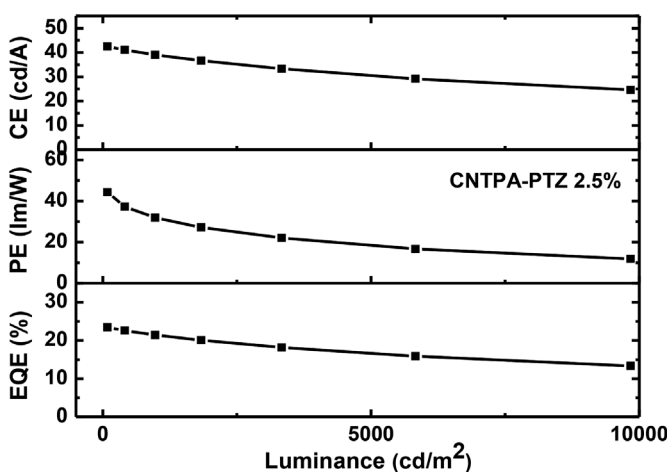
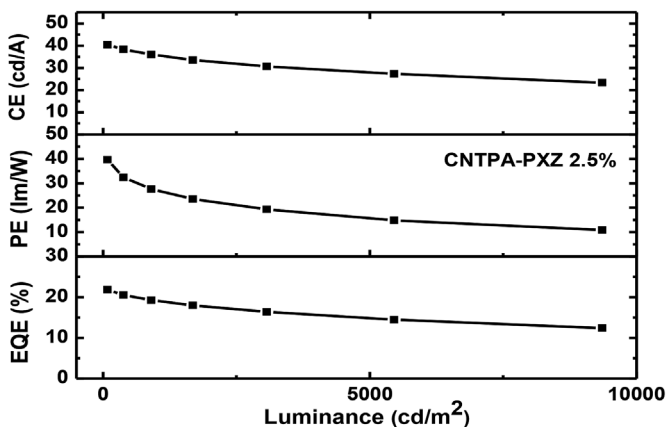
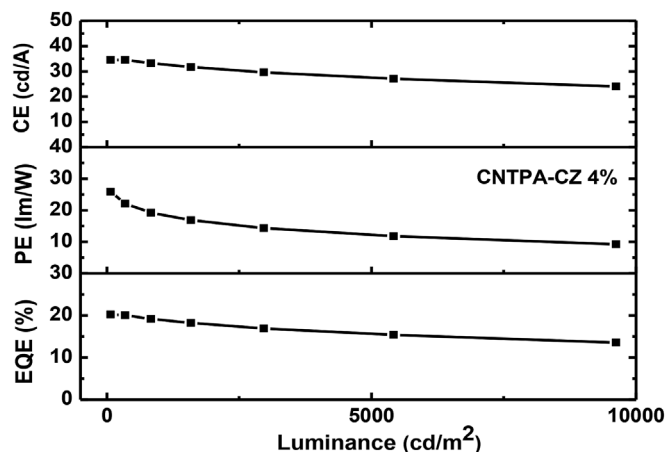


Fig. 8. The current efficiency (CE)-, power efficiency (PE)-, and external quantum efficiency (EQE)-luminance curves.

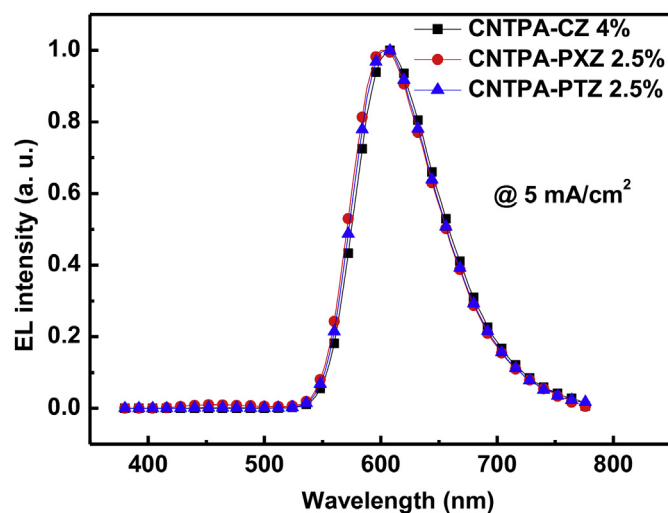


Fig. 9. The EL spectra of devices at 5 mA/cm².

devices showed superior performance compared to those based on CNTPA-CZ and CNTPA-PXZ with a maximum EQE of 23.5% and 21.4% at 1000 cd/m². The results indicated the great potential of this type of tripodal bipolar materials for the application in OLEDs.

Acknowledgements

We acknowledge the financial support from the National Key R&D Program of China (2016YFB0400703), the National Natural Science Foundation of China (21472135 and 61307036), Natural Science Foundation of Jiangsu Province of China (BK20151216), and the 111 Project. This project is also funded by Collaborative Innovation Center of Suzhou Nano Science and Technology (CIC-NANO), Soochow University and by the Priority Academic Program Development of Jiangsu Higher Education Institutions (PAPD).

Appendix A. Supplementary data

Supplementary data to this article can be found online at <https://doi.org/10.1016/j.dyepig.2018.10.076>.

References

- [1] Tang CW, VanSlyke SA. Organic electroluminescent diodes. *Appl Phys Lett* 1987;51:913–5.
- [2] Ma Y, Zhang H, Shen J, Che C. Electroluminescence from triplet metal–ligand charge-transfer excited state of transition metal complexes. *Synth Met* 1998;94:245–8.
- [3] Baldo MA, O'Brien DF, You Y, Shoustikov A, Sibley S, Thompson ME, et al. Highly efficient phosphorescent emission from organic electroluminescent devices. *Nature* 1998;395:151–4.
- [4] Cui L-S, Kim JU, Nomura H, Nakanotani H, Adachi C. Benzimidazobenzothiazole-base bipolar hosts to harvest nearly all of the excitons from blue delayed fluorescence and phosphorescent organic light-emitting diodes. *Angew Chem Int Ed* 2016;55:6864–8.
- [5] Ma D, Tsuboi T, Qiu Y, Duan L. Recent progress in ionic iridium(III) complexes for organic electronic devices. *Adv Mater (Weinheim, Ger)* 2017;29:1603253.
- [6] Ho C-L, Wong W-Y. Charge and energy transfers in functional metallophosphors and metallopolynes. *Coord Chem Rev* 2013;257:1614–49.
- [7] Uoyama H, Goushi K, Shizu K, Nomura H, Adachi C. Highly efficient organic light-emitting diodes from delayed fluorescence. *Nature* 2012;492:234–8.
- [8] Cleave V, Yahioğlu G, Barny PL, Friend RH, Tessler N. Harvesting singlet and triplet energy in polymer LEDs. *Adv Mater (Weinheim, Ger)* 1999;11:285–8.
- [9] Zhou Y-H, Xu J, Wu Z-G, Zheng Y-X. Synthesis, photoluminescence and electroluminescence of one iridium complex with 2-(2,4-difluorophenyl)-4-(trifluoromethyl)pyrimidine and tetraphenylimidodiphosphinate ligands. *J Organomet Chem* 2017;848:226–31.
- [10] Xia D, Wang B, Chen B, Wang S, Zhang B, Ding J, et al. Self-host blue-emitting iridium dendrimer with carbazole dendrons: nonpopped phosphorescent organic light-emitting diodes. *Angew Chem* 2014;126:1066–70.
- [11] Zhou G, Ho C-L, Wong W-Y, Wang Q, Ma D, Wang L, et al. Manipulating charge-

- transfer character with electron-withdrawing main-group moieties for the color tuning of iridium electrophosphors. *Adv Funct Mater* 2008;18:499–511.
- [12] Yeh S-J, Wu M-F, Chen C-T, Song Y-H, Chi Y, Ho M-H, et al. New dopant and host materials for blue-light-emitting phosphorescent organic electroluminescent devices. *Adv Mater (Weinheim, Ger)* 2005;17:285–9.
- [13] Cai X, Gao B, Li X-L, Cao Y, Su S-J. Singlet–triplet splitting energy management via acceptor substitution: complanation molecular design for deep-blue thermally activated delayed fluorescence emitters and organic light-emitting diodes application. *Adv Funct Mater* 2016;26:8042–52.
- [14] Liu M, Komatsu R, Cai X, Sasabe H, Kamata T, Nakao K, et al. Introduction of twisted backbone: a new strategy to achieve efficient blue fluorescence emitter with delayed emission. *Adv Optical Mater* 2017;1700334.
- [15] Lin B-Y, Easley CJ, Chen C-H, Tseng P-C, Lee M-Z, Sher P-H, et al. Exciplex-sensitized triplet–triplet annihilation in heterojunction organic thin-film. *ACS Appl Mater Interfaces* 2017;9:10963–70.
- [16] Moon C-K, Suzuki K, Shizu K, Adachi C, Kaji H, Kim J-J. Combined inter- and intramolecular charge-transfer processes for highly efficient phosphorescent organic light-emitting diodes with reduced triplet exciton quenching. *Adv Mater (Weinheim, Ger)* 2017;29:1606448.
- [17] Zhao J, Yang Z, Chen X, Xie Z, Liu T, Chi Z, et al. Efficient triplet harvesting in fluorescence–TADF hybrid warm-white organic light-emitting diodes with a fully non-doped device configuration. *J Mater Chem C* 2018;6:4257–64.
- [18] Liu X-Y, Tang X, Zhao Y, Zhao D, Fan J, Liao L-S. Dispiro and propellane: novel molecular platforms for highly efficient organic light-emitting diodes. *ACS Appl Mater Interfaces* 2018;10:1925–32.
- [19] Li J, Li Y-H, Zhao Y, Liu X-Y, Fung M-K, Fan J. Naphthalene-based host materials for highly efficient red phosphorescent OLEDs at low doping ratios. *Org Electron* 2018;54:140–7.
- [20] Liu X-Y, Tang X, Zhao Y, Zhao D, Fan J, Liao L-S. Spiro[bibenzofuran][4,4]azaline: a novel platform for host materials in highly efficient organic light-emitting diodes. *J Mater Chem C* 2018;6:1023–30.
- [21] Liu X-Y, Tian Q-S, Zhao D, Fan J, Liao L-S. Novel o-D- π -A arylamine/arylphosphine oxide hybrid hosts for efficient phosphorescent organic light-emitting diodes. *Org Electron* 2018;56:186–91.
- [22] Hu Y, Yuan Y, Shi Y-L, Lin J-D, Jiang Z-Q, Liao L-S. Efficient near-infrared organic light-emitting diodes based on a bipolar host. *J Mater Chem C* 2018;6:1407–12.
- [23] Li W, Zhao J, Li L, Du X, Fan C, Zheng C, et al. Efficient solution-processed blue and white OLEDs based on a high-triplet bipolar host and a blue TADF emitter. *Org Electron* 2018;58:276–82.
- [24] Wang F, Liu D, Li J, Ma M. Modulation of n-type units in bipolar host materials toward high-performance phosphorescent OLEDs. *ACS Appl Mater Interfaces* 2017;9:37888–97.
- [25] Park IS, Seo H, Tachibana H, Kim JU, Zhang J, Son SM, et al. Cyclohexane-coupled bipolar host materials with high triplet energies for organic light-emitting diodes based on thermally activated delayed fluorescence. *ACS Appl Mater Interfaces* 2017;9:2693–700.
- [26] Chaskar A, Chen H-F, Wong K-T. Bipolar host materials: a chemical approach for highly efficient electrophosphorescent devices. *Adv Mater (Weinheim, Ger)* 2011;23:3876–95.
- [27] Kim D, Coropceanu V, Brédas J-L. Design of efficient ambipolar host materials for organic blue electrophosphorescence: theoretical characterization of hosts based on carbazole derivatives. *J Am Chem Soc* 2011;133:17895–900.
- [28] Zheng C-J, Ye J, Lo M-F, Fung M-K, Ou X-M, Zhang X-H, et al. New ambipolar hosts based on carbazole and 4,5-diazafluorene units for highly efficient blue phosphorescent OLEDs with low efficiency roll-off. *Chem Mater* 2012;24:643–50.
- [29] Zhou H-H, Cheng C-H. A highly efficient universal bipolar host for blue, green, and red phosphorescent OLEDs. *Adv Mater (Weinheim, Ger)* 2010;22:2468–71.
- [30] Hsu F-M, Chien C-H, Shih P-I, Shu C-F. Phosphine-oxide-containing bipolar host material for blue electrophosphorescent devices. *Chem Mater* 2009;21:1017–22.
- [31] Lee CW, Lee JY. High quantum efficiency in solution and vacuum processed blue phosphorescent organic light emitting diodes using a novel benzofuroiridine-based bipolar host material. *Adv Mater (Weinheim, Ger)* 2013;25:596–600.
- [32] Chen J, Shi C, Fu Q, Zhao F, Hu Y, Feng Y, et al. Solution-processable small molecules as efficient universal bipolar host for blue, green and red phosphorescent inverted OLEDs. *J Mater Chem* 2012;22:5164–70.
- [33] Chien C-H, Hsu F-M, Shu C-F, Chi Y. Efficient red electrophosphorescence from a fluorene-based bipolar host material. *Org Electron* 2009;10:871–6.
- [34] Pan B, Wang B, Wang Y, Xu P, Wang L, Chen J, et al. A simple carbazole-N-benzimidazole bipolar host material for highly efficient blue and single layer white phosphorescent organic light-emitting diodes. *J Mater Chem C* 2014;2:2466–9.
- [35] Lee J-H, Shin H, Kim J-M, Kim K-H, Kim J-J. Exciplex-forming Co-Host-Based red phosphorescent organic light-emitting diodes with long operational stability and high efficiency. *ACS Appl Mater Interfaces* 2017;9:3277–81.
- [36] Wang Y-K, Li S-H, Wu S-F, Huang C-C, Kumar S, Jiang Z-Q, et al. Tilted spiro-type thermally activated delayed fluorescence host for $\approx 100\%$ exciton harvesting in red phosphorescent electronics with ultralow doping ratio. *Adv Funct Mater* 2018;28:1706228.
- [37] Fleetham T, Li G, Wen L, Li J. Efficient “pure” blue OLEDs employing tetradentate Pt complexes with a narrow spectral bandwidth. *Adv Mater (Weinheim, Ger)* 2014;26:7116–21.
- [38] Fan C-H, Sun P, Su T-H, Cheng C-H. Host and dopant materials for idealized deep-red organic electrophosphorescence devices. *Adv Mater (Weinheim, Ger)* 2011;23:2981–5.
- [39] Lamansky S, Djurovich P, Murphy D, Abdel-Razzaq F, Lee H-E, Adachi C, et al. Highly phosphorescent bis-cyclometalated iridium complexes: synthesis, photophysical characterization, and use in organic light emitting diodes. *J Am Chem Soc*

- 2001;123:4304–12.
- [40] Han C, Zhao Y, Xu H, Chen J, Deng Z, Ma D, et al. A simple phosphine–oxide host with a multi-insulating structure: high triplet energy level for efficient blue electrophosphorescence. *Chem Eur J* 2011;17:5800–3.
- [41] Reineke S, Lindner F, Schwartz G, Seidler N, Walzer K, Lüssem B, et al. White organic light-emitting diodes with fluorescent tube efficiency. *Nature* 2009;459:234–8.
- [42] Wu M-F, Yeh S-J, Chen C-T, Murayama H, Tsuboi T, Li W-S, et al. The quest for high-performance host materials for electrophosphorescent blue dopants. *Adv Funct Mater* 2008;17:1887–95.
- [43] Tsuboi T, Liu S-W, Wu M-F, Chen C-T. Spectroscopic and electrical characteristics of highly efficient tetraphenylsilane-carbazole organic compound as host material for blue organic light emitting diodes. *Org Electron* 2009;10:1372–7.
- [44] Kim M, Jeon SK, Hwang S-H, Lee JY. Stable blue thermally activated delayed fluorescent organic light-emitting diodes with three times longer lifetime than phosphorescent organic light-emitting diodes. *Adv Mater (Weinheim, Ger)* 2015;27:2515–20.
- [45] Kim JH, Yoon DY, Kim JW, Kim J-J. New host materials with high triplet energy level for blue-emitting electrophosphorescent device. *Synth Met* 2007;157:743–50.
- [46] Zhang Y, Haske W, Cai D, Barlow S, Kippelen B, Marder SR. Efficient blue-emitting electrophosphorescent organic light-emitting diodes using 2-(3,5-di(carbazol-9-yl)phenyl)-5-phenyl-1,3,4-oxadiazole as an ambipolar host. *RSC Adv* 2013;3:23514–20.
- [47] Rajamalli P, Senthilkumar N, Gandeepan P, Ren-Wu C-Z, Lin H-W, Cheng C-H. A thermally activated delayed blue fluorescent emitter with reversible externally tunable emission. *J Mater Chem C* 2016;4:900–4.
- [48] Cho YJ, Lee JY. Modified N,N'-Dicarbazolyl-3,5-benzene as a high triplet energy host material for deep-blue phosphorescent organic light-emitting diodes. *Chem Eur J* 2011;17:11415–8.
- [49] Gaj MP, Fuentes-Hernandez C, Zhang Y, Marder SR, Kippelen B. Highly efficient Organic Light-Emitting Diodes from thermally activated delayed fluorescence using a sulfone–carbazole host material. *Org Electron* 2015;16:109–12.
- [50] Tanaka H, Shizu K, Nakanotani H, Adachi C. Twisted intramolecular charge transfer state for long-wavelength thermally activated delayed fluorescence. *Chem Mater* 2013;25:3766–71.
- [51] Bian C, Wang Q, Liu X-Y, Fan J, Liao L-S. Orthogonally substituted aryl derivatives as bipolar hosts for blue phosphorescent organic light-emitting diodes. *Org Electron* 2017;46:105–14.
- [52] Schwartz G, Pfeiffer M, Reineke S, Walzer K, Leo K. Harvesting triplet excitons from fluorescent blue emitters in white organic light-emitting diodes. *Adv Mater (Weinheim, Ger)* 2007;19:3672–6.
- [53] Sun X, Liu Y, Chen S, Qiu W, Yu G, Ma Y, et al. X-shaped electroactive molecular materials based on oligothiophene architectures: facile synthesis and photophysical and electrochemical properties. *Adv Funct Mater* 2006;16:917–25.
- [54] Sun J, Jiang H-j, Zhang J-l, Tao Y, Chen R-f. Synthesis and characterization of heteroatom substituted carbazole derivatives: potential host materials for phosphorescent organic light-emitting diodes. *New J Chem* 2013;37:977–85.
- [55] Chen X-K, Tsuchiya Y, Ishikawa Y, Zhong C, Adachi C, Brédas J-L. A new design strategy for efficient thermally activated delayed fluorescence organic emitters: from twisted to planar structures. *Adv Mater (Weinheim, Ger)* 2017;29:1702767.
- [56] Sasabe H, Toyota N, Nakanishi H, Ishizaka T, Pu Y-J, Kido J. 3,3'-Bicarbazole-Based host materials for high-efficiency blue phosphorescent OLEDs with extremely low driving voltage. *Adv Mater (Weinheim, Ger)* 2012;24:3212–7.